

Failure Physics and Reliability of GaN-Based HEMTs for Microwave and Millimeter-Wave Applications: A Review of Consolidated Data and Recent Results

Enrico Zanoni,* Fabiana Rampazzo, Carlo De Santi, Zhan Gao, Chandan Sharma, Nicola Modolo, Giovanni Verzellesi, Alessandro Chini, Gaudenzio Meneghesso, and Matteo Meneghini

Herein, the results are reviewed concerning reliability of high-electron mobility transistors (HEMTs) based on GaN, which currently represent the technology of choice for high-efficiency microwave and millimeter-wave power amplifiers. Several failure mechanisms of these devices are extensively studied, including converse piezoelectric effects, formation of conductive percolation paths at the edge of gate toward the drain, surface oxidation of GaN, time-dependent breakdown of GaN buffer, and of field-plate dielectric. For GaN HEMTs with scaled gate length, the simultaneous control of short-channel effects, deep-level dispersion, and hot-electron-induced degradation requires a careful optimization of epitaxial material quality and device design.


1. Introduction

The properties of gallium nitride are extremely favorable for the design of high-frequency power devices: a high breakdown

E. Zanoni, F. Rampazzo, C. De Santi, Z. Gao, C. Sharma, N. Modolo, G. Meneghesso, M. Meneghini
Department of Information Engineering
University of Padova
via Gradenigo 6/B, 35131 Padova, Italy
E-mail: enrico.zanoni@dei.unipd.it

G. Verzellesi
Department of Engineering Science and Methods
University of Modena and Reggio Emilia
via Amendola 2 - Pad. Morselli
42122 Reggio Emilia, Italy

A. Chini
Department of Engineering "Enzo Ferrari"
University of Modena and Reggio Emilia
Via P. Vivarelli 10
41125 Modena, Italy

 The ORCID identification number(s) for the author(s) of this article can be found under <https://doi.org/10.1002/pssa.202100722>.

© 2022 The Authors. physica status solidi (a) applications and materials science published by Wiley-VCH GmbH. This is an open access article under the terms of the Creative Commons Attribution-NonCommercial License, which permits use, distribution and reproduction in any medium, provided the original work is properly cited and is not used for commercial purposes.

DOI: 10.1002/pssa.202100722

voltage can be achieved thanks to the wide energy gap, which effectively suppresses electron-hole pair generation due to impact ionization and increases breakdown voltage; a high electron saturation velocity ($>3 \times 10^7 \text{ cm s}^{-1}$) and electron mobility is coupled with the highest possible electron density in the 2D electron gas (2DEG). Correspondingly, current and power density are much higher than in Si or GaAs devices, which translates into reduced width and area (thus reducing parasitics and greatly increasing efficiency). The wider bandgap provides high robustness against various types of electrical overstress (DC, electrostatic discharge, radiofrequency (RF)), and a wider dynamic range, better linearity, and higher operating temperature.

RF power performance of Ga-polar GaN HEMTs for microwave and millimeter-wave applications was recently reviewed^[1]; power densities as high as 4 W mm^{-1} at 38 GHz and 2.8 W mm^{-1} at 95 GHz have been demonstrated.^[2,3]

In absence of viable and cost-competitive bulk GaN substrates, RF GaN HEMTs are usually based on GaN-on-SiC epitaxial layers; GaN-on-Si is also becoming popular for lower frequency applications, thanks to its reduced cost and larger wafer size. Substrate isolation is achieved by introducing a GaN "buffer" layer, doped with Fe or C (or both); however, these dopants are associated with GaN lattice defects, which may enhance deep-level effects.^[4,5] Lateral gate length scaling, needed to achieve high cutoff and oscillation frequency values, requires a reduced vertical distance between gate and channel. A reduction in the barrier thickness would lower the 2DEG charge carrier density; a redesign of the HEMT structure is therefore needed. For sub-100 nm gate lengths, several new device designs have been proposed, adopting higher bandgap barrier layers such as InAl(Ga)N, and/or double heterojunctions.^[1]

A radical solution to scaling-related issues consists in the adoption of nitrogen-polar epitaxial structures, where the GaN channel is on top and the AlGaIn layer underneath inherently acts as a back-barrier; low ohmic contact resistance on GaN is achieved and scalability is greatly improved.^[6] Consequently, nitrogen-polar HEMTs have reached record values of power density and power-added efficiency (PAE): stable 8 W mm^{-1} from 10 to 94 GHz^[7]; 10.3 W mm^{-1} at 30 GHz with 47.4% PAE^[8];

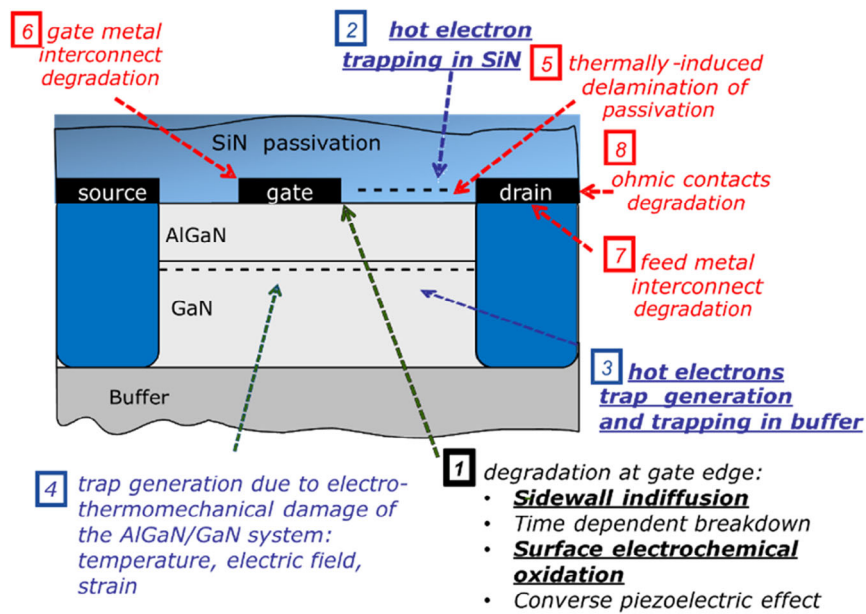


Figure 1. Schematic cross section of an AlGaIn/GaN high electron mobility transistors (HEMT) showing the most common failure mechanisms described in the literature.

6.2 W mm^{-1} and record 33.8% PAE at 94 GHz adopting atomic layer deposition of Ru Schottky contacts and a deep-recess metal-insulator-semiconductor HEMT (MISHEMT) structure.^[9]

GaN microwave HEMTs have also unique reliability issues, related to material properties and epitaxial growth quality.^[10–15]

Figure 1 shows a schematic cross section of an AlGaIn/GaN HEMTs and lists main failure mechanisms reported in the literature, which are shortly summarized in the following. The main goal of this paper is not to provide a comprehensive discussion on all the possible degradation mechanisms, but only to highlight some of the most recent findings that are relevant for state-of-the-art devices and for future development. More information and a more detailed discussion on the reviewed papers can be found in the corresponding references.

1.1. Inverse Piezoelectric Effect and Thermomechanical Strain

The most critical area in a GaN HEMT is located in the semiconductor layers at the drain side of the gate edge, where the maximum current density, electric field, and local temperature are present at the same time. In this position, several degradation mechanisms are accelerated: due to the piezoelectric nature of GaN, the presence of an electric field implies an enhancement of tensile stress in the AlGaIn barrier, which is relaxed through the creation of lattice defects or even cracks, resulting in degradation in drain current, I_D , and increase in gate leakage current, I_G . Even in the absence of applied bias, thermal cycling at high temperature (300–650 K) can also induce cracks due to thermal mismatch between GaN, gate metallization, and Si_xN_y passivation. Thermomechanical strain concentrates at the gate edges and is symmetrical with respect to the gate center, thus leading to crystal damage both at source and drain side, see **Figure 2**.^[16,17]

1.2. Time-Dependent Breakdown of the AlGaIn/GaN Structure and of Dielectrics

Due to the polar nature of chemical bonds in GaN, defects may be generated under the action of the intense electric field and become organized in a conducting percolative path, causing a sudden increase in I_G . The kinetic of this degradation is compatible with a time-dependent dielectric breakdown (TDDB) mechanism: during a test at constant voltage in the offstate, initially the gate current becomes noisy, then it suddenly increases several orders of magnitude.^[18–21] The conductive path forms on the device surface at the gate edge and can be located by electroluminescence (EL) microscopy^[21]; the actual observation of the damaged region, which has a typical extension of few nanometers, requires careful sample preparation and the use of transmission electron microscopy (TEM). It can even be elusive, if the leakage is just due to a percolative chain of point defects, which are not detectable by TEM. These time-dependent breakdown effects are peculiar to polar semiconductors such as GaN, and have been observed also in InGaIn/GaN light-emitting diodes submitted to reverse bias tests.^[22]

Due to the high electric field present in the device, dielectrics are also subject to intense stress and can be affected by TDDB mechanisms; in particular, a critical point is the dielectric below the gate field-plate edge.^[23–27]

1.3. Gate Metal, Contaminants, and Oxygen Interdiffusion: Electrochemical GaN Oxidation

Under the action of high temperature and high-electric field, gate metals and contaminants can diffuse toward the semiconductor surface, in particular at the sidewall interface between metal and

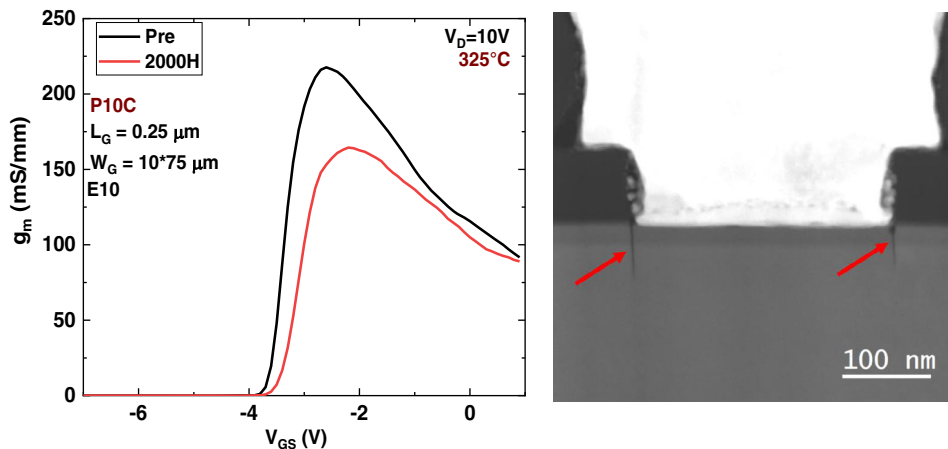


Figure 2. Left: transconductance g_m versus V_{GS} for a 0.25 μm AlGaIn/GaN HEMT before and after 2000 h of thermal storage at 325 $^{\circ}\text{C}$. Right: scanning transmission electron microscope (STEM) image of the cross section along gate length of gate contact after test, showing the presence of two cracks at gate edges at the source and drain side.

passivation (usually Si_xN_y); interdiffusion of Au, O, and other elements has been observed.^[28–31] In specific conditions (presence of moisture, high temperature, high electric field, device current), oxygen can react with GaN at the device surface, thus inducing pits and voids close to gate edges, with increase in the parasitic resistance of access regions and decrease in transconductance.

Electrochemical dissolution of GaN can lead to progressive structural damage at the drain edge of the gate, consisting in the formation of pits and grooves, associated with the presence of oxygen or water vapor, leading to the formation of Ga and Al oxide.^[32,33] A relatively complex chain of electrochemical reactions, which requires the presence of holes generated by band-to-band tunneling, has been identified as a possible mechanism for GaN surface oxidation. Other authors observed the formation of an interfacial layer under the gate contact, composed by an amorphous layer of aluminum oxide, which is formed from the rejection of N and the consumption of Al from an as-formed interfacial layer composed of Al, Ga, O, and N.^[34,35]

Schottky and ohmic contacts on GaN and related compounds are generally stable at high temperature.^[36] Both Schottky and ohmic contact can withstand 300 $^{\circ}\text{C}$ for extended periods, even if Ni has been reported to form NiO- and Ni-nitrides starting at annealing temperatures as low as 200 $^{\circ}\text{C}$.

1.4. Deep Levels and Hot-Electron Effects

Permanent and recoverable trapping and detrapping effects may lead to significant device drift, with change in the threshold voltage and transconductance. These may be due to material quality (preexisting deep levels on the surface and at interfaces, within the GaN buffer, within the semi-insulating substrate), or to process-induced instabilities, especially in connection with compensating species (Fe or C), contaminants like H, F, O, or defects.^[5] Hot-electron effects, with generation of deep levels and trapping of electrons in the dielectrics or/and at surfaces and interfaces under the gate as over the gate–drain access

region, may occur both during off-state tests or (more frequently) during semi-on and on-state tests.^[37–42]

The term “hot electrons” refers to nonequilibrium electrons, which acquire kinetic energy values sufficient to overcome potential energy barriers, be injected into buffer, barrier, or insulating layers and be trapped there, break atomic bonds, and create interface states or activate traps, for instance, through dehydrogenation, see **Figure 3**.^[40,43,44] According to the various experimental conditions, material properties, and device weaknesses, hot electrons may give rise both to parametric, gradual, permanent, or recoverable positive or negative threshold voltage shifts and/or to decrease in transconductance.

In Si n-MOSFET, holes generated by impact ionization can be collected as substrate current I_b ; in AlGaAs/GaAs HEMTs, impact ionization hole current induces a negative gate current I_g which can be correlated to hot-electron effects.^[45] Due to

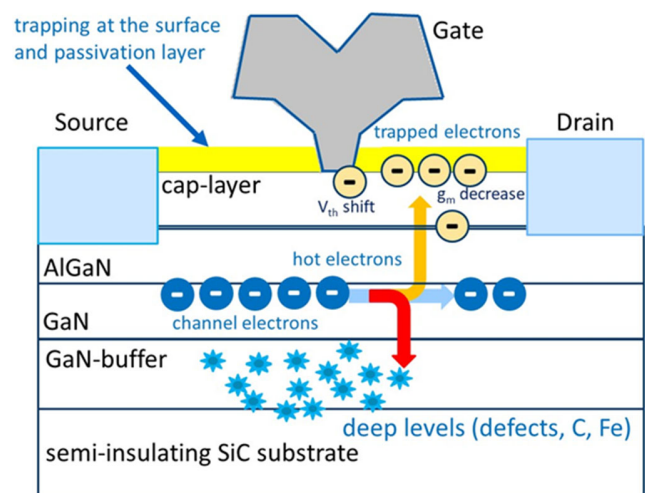


Figure 3. Schematic cross section of an AlGaIn/GaN HEMT showing possible effects of hot electrons: energetic electrons can be trapped at interfaces, within the GaN buffer, at surface or within passivation.

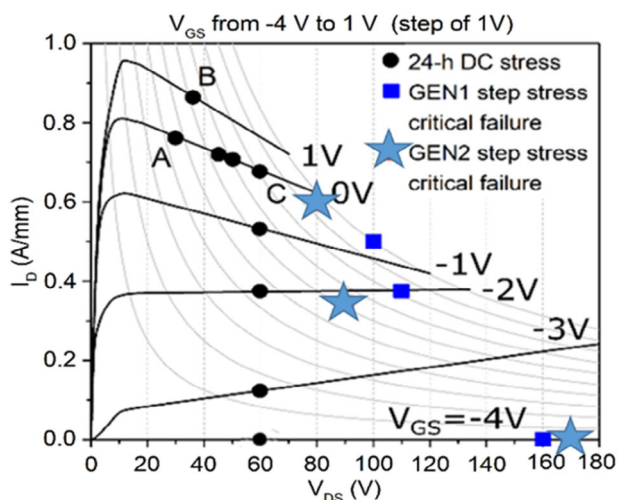


Figure 4. Representative I - V device characteristics showing bias points adopted for 24 h tests (circles). Breakdown voltage values are shown as squares (GEN1 devices) and stars (GEN2 devices). Reproduced with permission.^[48] Copyright 2020, IEEE.

the different leakage mechanisms present in a GaN HEMT, and to the wide bandgap reducing impact ionization effects, the gate current is not representative of hot-electron phenomena, unless the devices to be studied present an extremely low leakage current.^[46] The characterization of hot-electron effects in GaN HEMTs is usually based on the measurements of EL, due to intraband transitions of energetic electrons (Bremsstrahlung).^[13,47] EL has a non-monotonic behavior as a function of gate voltage: starting from pinch-off and increasing gate-source voltage (V_{GS}), EL first increases as 2DEG density in the channel is increased; at high V_{GS} , g_m saturates and EL decreases due to electric-field decrease at increasing V_{GS} . This feature can be exploited to verify if the failure mechanism is due to hot electrons, by checking if, at a given drain-source voltage (V_{DS}), the degradation has the same non-monotonic dependence on V_{GS} as EL.^[39]

2. Failure Mechanisms of RF GaN HEMTs: Three Case Studies

In the following, we describe three representative studies concerning failure mechanisms of RF GaN HEMTs: in Section 2.1, we show that short-term (<100 h) on-wafer testing of devices at various bias conditions can effectively detect HEMT weaknesses (in this case, due to sidewall indiffusion of Au and O followed by GaN oxidation), thus suggesting specific process changes. Hot-electron effects are the subject of case studies 2 and 3; in Section 2.2, we show that enhanced degradation may result from an intrinsic device weakness (incomplete pinch-off due to short-channel effects) coupled with particular electrical stress conditions consequent to RF testing in compression; finally, in Section 2.3, the dependence of hot-electron-induced degradation on GaN buffer compensation doping is discussed, and a hypothesis on a possible role of C accelerating the degradation is presented.

2.1. First Case Study: Gold and Oxygen Sidewall Interdiffusion and AlGaIn Surface Oxidation

The 0.25 μm GaN/AlGaIn/GaN HEMTs for microwave applications up to 20 GHz have been tested.^[48] Devices adopted a 22 nm AlGaIn barrier with 22% Al content and Ti/Al/Ni/Au ohmic contacts. Two different sets of devices were tested: 1) GEN1, adopting a Ni/Pt/Au Schottky gate metallization and standard plasma-enhanced chemical vapor deposition (PE-CVD) for SiN passivation; and 2) GEN2 devices, adopting a different gate metallization scheme and a double-layer SiN passivation.^[49,50]

Devices were submitted to 24 h on-wafer DC tests at various bias points, as shown in **Figure 4**. Significant degradation was observed in GEN1 devices when the applied DC power was larger than 20 W mm^{-1} . Degradation consisted in a decrease in drain current and transconductance decrease without changes in the threshold voltage, suggesting damage in the gate-drain access region, **Figure 5**.

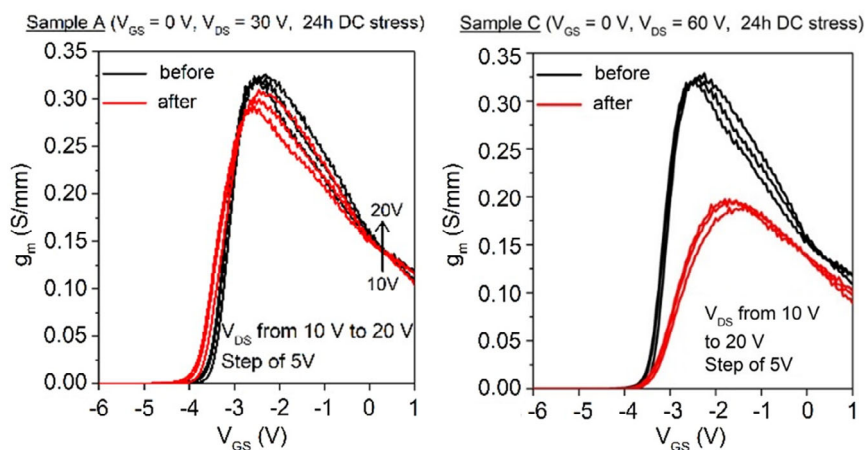


Figure 5. Left: transconductance g_m in a GEN1 HEMT before and after 24 h test at $V_{GS} = 0$ V, $V_{DS} = 30$ V; right: after 24 h at $V_{GS} = 0$ V, $V_{DS} = 60$ V. Reproduced with permission.^[48] Copyright 2020, IEEE.

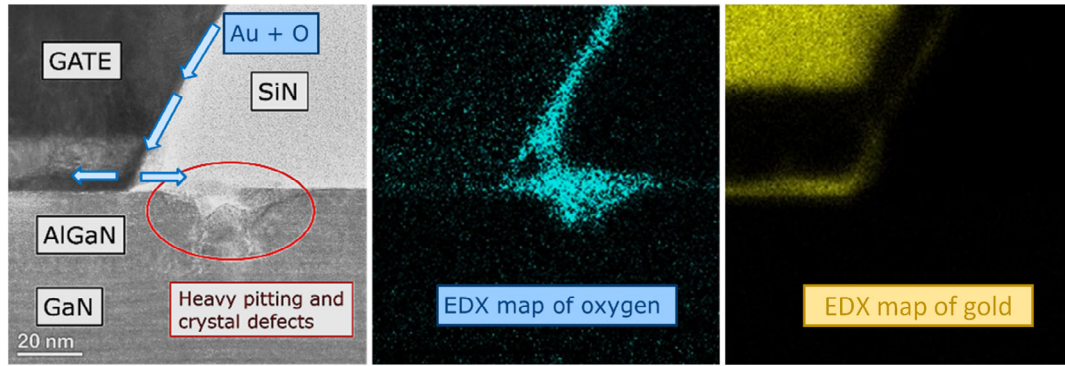


Figure 6. Left, STEM image of defect at the gate–drain access region. Energy-dispersive X-Ray (EDX) mapping of oxygen (center) and gold (right), after 24 h DC test at $V_{GS} = 1$ V, $V_{DS} = 38$ V, DC $P_D = 31$ W mm $^{-1}$, GEN1 device. Reproduced with permission.^[48] Copyright 2020, IEEE.

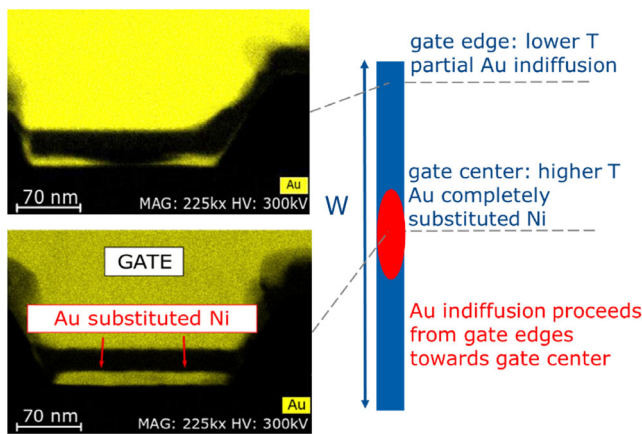


Figure 7. Left, top: EDX map of Au at the edge of gate width for a GEN1 0.25 μ m AlGaIn/GaN HEMT after 24 h test at $V_{GS} = 0$ V, $V_{DS} = 60$ V, DC $P_D = 35$ W mm $^{-1}$. Bottom, left: Au EDX map taken at the center of gate width. Reproduced with permission.^[48] Copyright 2020, IEEE.

Devices were then submitted to failure analysis using focused ion beam (FIB) cross sectioning, scanning TEM (STEM) imaging and EDX, shown in both **Figure 6** and **7**. X-Ray element microanalysis detected indiffusion of Au and O at the sidewall, within the interface between gate metal and SiN passivation. When oxygen reached the semiconductor surface, AlGaIn oxidation occurred, and heavy pitting and crystal damage, was induced, as shown in **Figure 6** (left). Both O and Au migrated over the AlGaIn surface toward the gate center and toward source and drain contact, as shown in **Figure 6** (center) and (right); Au gradually substituted Ni as Schottky contact, **Figure 7**.

In the device submitted to 24 h test at $V_{GS} = 0$ V, $V_{DS} = 60$ V, only partial lateral indiffusion of Au took place at the edges of the gate finger, while at the center of the finger, where temperature is higher, Au completely replaced Ni, as shown in **Figure 7**.

Figure 8 shows the percentage decrease in transconductance as a function of the estimated junction temperature T_j and demonstrates that the observed GaN oxidation is accelerated by the simultaneous action of high electric field, high temperature, and high current: no degradation occurs at room temperature (RT) in semi-on state at $V_{GS} = -3$ V, $V_{DS} = 60$ V (current + electric field + hot electrons, RT), or at 375 °C, without bias (high temperature

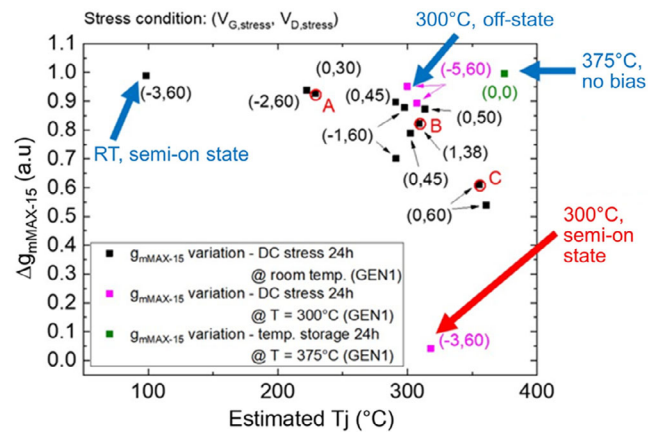


Figure 8. Percentage decrease of transconductance in GEN1 devices as a function of junction temperature during 24 h tests at various bias points. Degradation requires the simultaneous presence of high temperature, high electric field, and high current. In fact, devices tested at room temperature (RT) in semi-on-state, or at 300 °C in off-state, or at 375 °C without bias show no degradation. In GEN2 devices, with modified gate metal and passivation, g_m degradation is lower than 5% after 24 h test at $V_{GS} = 0$ V, $V_{DS} = 60$ V. Reproduced with permission.^[48] Copyright 2020, IEEE.

only), or at 300 °C in pinch-off (high temperature, high electric field, no current). Subsequent to the results of failure analysis, gate metallization was modified and a better passivation was introduced in GEN2 devices, improving sidewall morphology and achieving better stability; in GEN2 devices, g_m degradation is lower than 5% after 24 h test at $V_{GS} = 0$ V, $V_{DS} = 60$ V.

2.2. Second Case Study: Effect of Subthreshold Characteristics on Device Degradation during RF Tests

During RF tests, depending on the actual load line adopted, the device is repeatedly subject to bias conditions, which would not be sustainable during DC tests. In the semi-on region close to pinch-off, severe degradation due to hot electrons may occur, due to the simultaneous presence of high electric field and channel current. Depending on device characteristics, load line, and class of operation, this effect may induce significant reliability

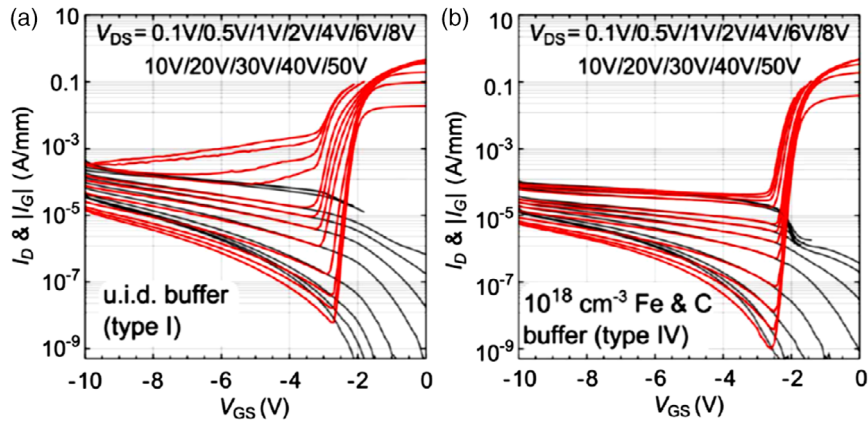


Figure 9. Subthreshold characteristics of device submitted to 24 h RF tests at $V_{DS} = 30$ V, class A, 6 dB compression. Left: device without intentional doping in the GaN buffer. Right: device with 10^{18} cm^{-3} Fe + C in the buffer. In the latter device, drain–source leakage in pinch-off conditions is effectively suppressed. Reproduced with permission.^[42] Copyright 2015, IEEE.

issues, which can remain undetected if only DC reliability testing is used. In this case study, we compare hot electron effects in $0.5 \mu\text{m}$ AlGaIn/GaN HEMTs having different GaN buffer compensation options, namely: no doping (type I), 10^{17} cm^{-3} C-doping (type II), 10^{17} cm^{-3} Fe doping (type III), or 10^{18} cm^{-3} Fe and 10^{18} cm^{-3} C co-doping (type IV).^[42] Devices were subjected to a 24 h continuous wave RF test at 2.5 GHz with quiescent bias at $V_{DS} = 30$ V, $I_D = 30\% I_{DSS}$, and driven into a 6 dB compression point. Baseplate temperature was set to 40°C . Devices with undoped buffer show poor subthreshold characteristics and incomplete pinch-off, with large drain–source leakage current (Figure 9); on the contrary, Fe and C co-doping was very effective in obtaining steep subthreshold slope, low drain-induced barrier lowering (DIBL), and good pinch-off characteristics with reduced drain–source leakage. When submitted

to RF testing, degradation in RF output power occurred, correlated with initial subthreshold drain–source leakage current, see Figure 10. No correlation is found between power dissipated during the RF stress and the degradation in the RF output power.

When parasitic GaN buffer conductivity is not controlled due to incomplete compensation, drain–source current leakage is maintained beyond pinch-off, generating a high density of highly energetic carriers or hot electrons, which can induce defects in the AlGaIn or GaN layers, through the direct damage of weak lattice bonds or the dehydrogenation of Ga vacancies or N antisites complexes.^[51,52] The effect of deep levels can be evaluated by means of pulsed IV transconductance measurements, as shown in Figure 11 (top). A drop in dynamic g_m at high V_{GS} without threshold shift is observed in devices with undoped buffer (Figure 11 (top left)), suggesting generation of traps in the gate–drain region. Deep levels can be identified by drain-current transient spectroscopy (DCTS), which shows that the worsening in current-collapse in devices without doping in the GaN buffer (the same occurs for C-doped buffer devices) is caused by an increase in two traps with an activation energy $E_A = 0.79$ eV and capture cross section $\sigma_c = 6 \times 10^{-13} \text{ cm}^{-2}$ (E3) and with $E_A = 0.84$ eV and capture cross section $\sigma_c = 4 \times 10^{-14} \text{ cm}^{-2}$ (E4) (Figure 11 [bottom left]).^[5] Devices with Fe and C co-doping show higher initial current collapse, mainly due to the Fe-related trap at $E_A = 0.56$ eV, $\sigma_c = 5 \times 10^{-15} \text{ cm}^{-2}$ (E2), but trap density does not increase after RF testing. In conclusion, hot-electron degradation of GaN HEMTs depends on device subthreshold characteristics and off-state leakage current; Fe and C co-doping is effective in reducing short-channel effects and preventing RF degradation, but at the expenses of an increased current collapse of the untreated devices. In undoped and C-doped devices, hot-electron degradation is due to the increase in density of traps having activation energies $E_A = 0.79$ and 0.84 eV.

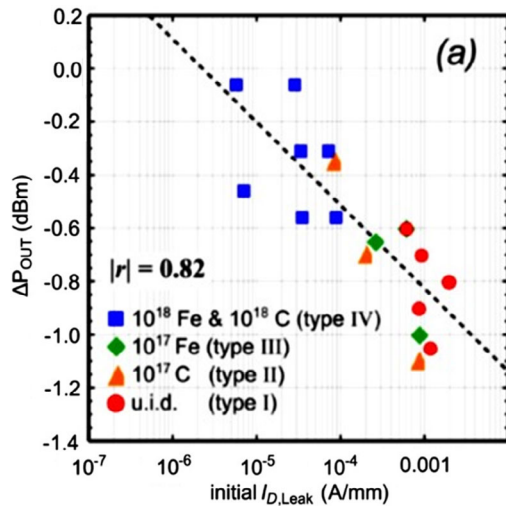


Figure 10. Degradation after 24 h RF test is directly correlated with drain–source current leakage in off-state at ($V_{GS} = V_{TH} - 1$ V, $V_{DS} = 40$ V). No correlation is found between power dissipated during the RF stress and the degradation in the RF output power. Reproduced with permission.^[42] Copyright 2015, IEEE.

2.3. Third Case Study: Effect of C-Doping on Short-Term GaN HEMTs Reliability

If on one hand C-doping or C + Fe co-doping can help in improving subthreshold characteristics and device reliability during RF

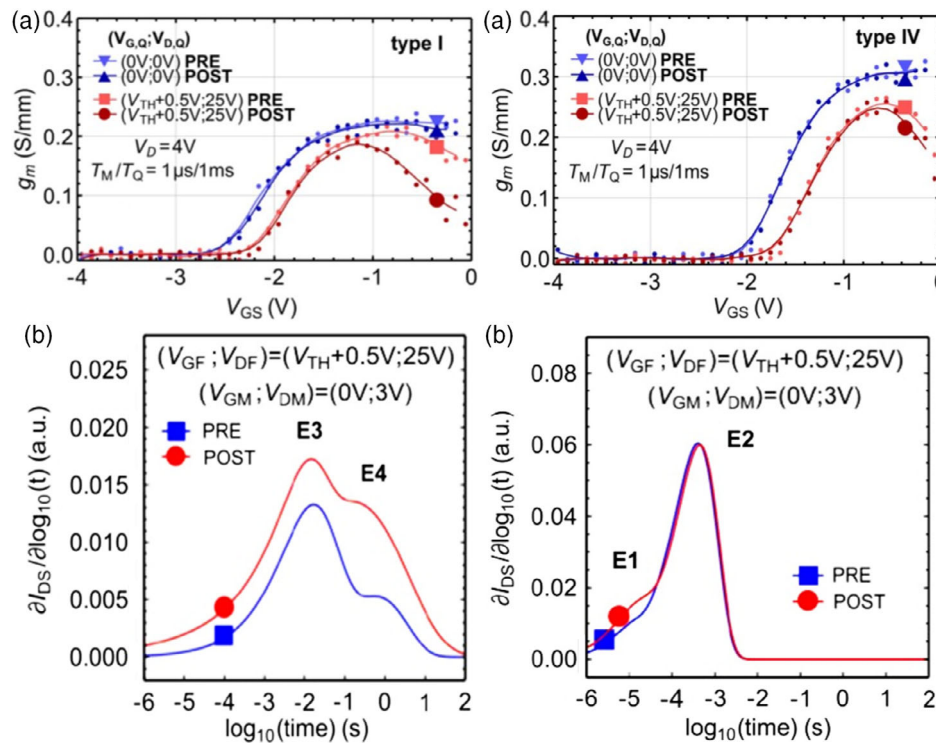


Figure 11. Left column, top: 24 h tests of devices with undoped GaN buffer induce a decrease in pulsed transconductance, in particular at high drain currents. Bottom: Drain Current Transient Spectroscopy reveals a strong increase in the concentration of the E4 trap, and a moderate increase of E3. Right column, top: in the devices with C + Fe co-doping, the pulsed g_m decrease is negligible, and correspondingly, the drain current transient spectroscopy (DCTS) spectra is unchanged (bottom). Reproduced with permission.^[42] Copyright 2015, IEEE.

stress, on the other hand, carbon introduces additional trapping sites, which may affect short-term device reliability. In fact, when C atoms occupy N sites, C_N , this defect behaves like an acceptor level at approximately 0.8 eV from the valence band. When these acceptors become ionized, they are negatively charged, inducing a backgating effect, which reduces I_D ; the recovery is slow because compensating holes need to be generated and brought back to the acceptors, resulting in frequency dispersion effects with long time constants.^[5,49,53] Moreover, hot electrons may interact with deep acceptor levels, and get trapped there, thus inducing a permanent or semi-permanent degradation in threshold voltage and I_D .

Three groups of 0.15 μm AlGaIn/GaN HEMTs were manufactured within the same industrial process, same batch but epitaxial layers differing for what concerns GaN buffer compensation doping, namely $a \ll \text{Fe reference} \gg$ wafer having $\text{Fe} = 2 \times 10^{18} \text{ cm}^{-3}$ and no C; $a \ll \text{Fe + low C} \gg$ wafer with $\text{Fe} = 2 \times 10^{18} \text{ cm}^{-3}$ and $\text{C} = 2 \times 10^{16} \text{ cm}^{-3}$; $a \ll \text{Fe + high C} \gg$ wafer with $\text{Fe} = 2 \times 10^{18} \text{ cm}^{-3}$ and $\text{C} = 8 \times 10^{16} \text{ cm}^{-3}$.^[50] These devices were submitted to step-stress tests in semi-on condition at $V_{GS} = -2 \text{ V}$ (the bias point was chosen in correspondence of the maximum EL emission, i.e., maximizing the effect of hot electrons), at increasing V_{DS} from 5 V in 5 V steps, 120 s each (Figure 12). Subsequently, fresh devices were submitted to 24 h tests at $V_{GS} = -2 \text{ V}$ and $V_{DS} = 25 \text{ V}$ (Figure 13).

For both types of tests, the degradation in drain current is maximum for the $\ll \text{Fe + high C} \gg$ devices, while it is

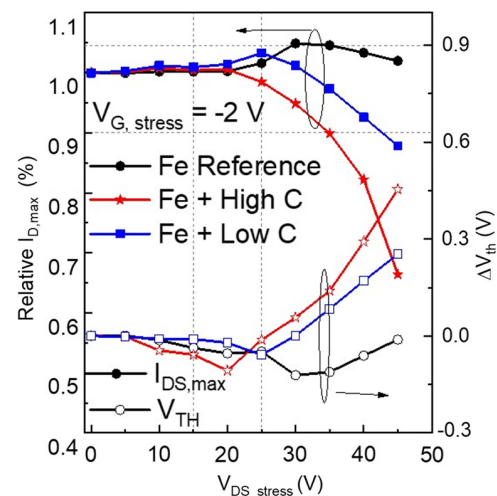


Figure 12. Drain current degradation and positive threshold voltage shift in different 0.15 μm AlGaIn/GaN HEMTs manufactured within the same process, same batch, but differing for the GaN buffer doping: Fe reference $\rightarrow \text{Fe} = 2 \times 10^{18} \text{ cm}^{-3}$, no C; Fe + low C $\rightarrow \text{Fe} = 2 \times 10^{18} \text{ cm}^{-3}$, $\text{C} = 2 \times 10^{16} \text{ cm}^{-3}$; Fe + high C $\rightarrow \text{Fe} = 2 \times 10^{18} \text{ cm}^{-3}$, $\text{C} = 8 \times 10^{16} \text{ cm}^{-3}$. Semi-on step-stress test at $V_{GS} = -2 \text{ V}$, increasing V_{DS} starting from 5 V in 5 V steps, 120 s each. Faster degradation is observed in Fe + high C-doped devices. Reference devices (Fe only) show negligible degradation (slight I_D increase due to negative V_{TH} shift), ruling out possible thermally activated interdiffusion effects. Reproduced with permission.^[54] Copyright 2020, Elsevier.

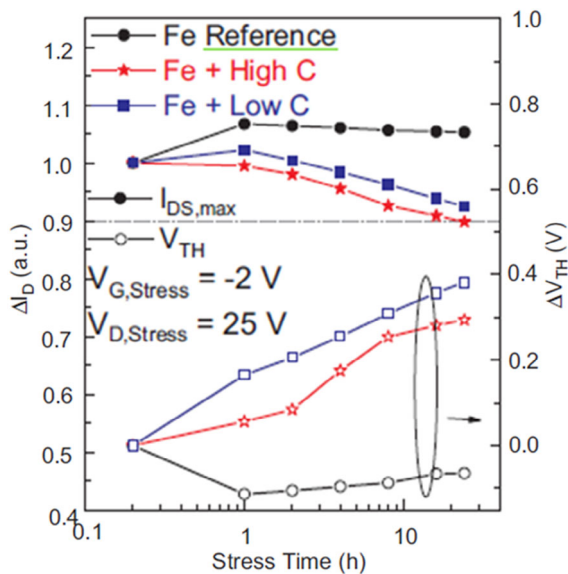


Figure 13. Drain current degradation and positive threshold voltage shift in different $0.15\ \mu\text{m}$ AlGaIn/GaN HEMTs manufactured within the same process, same batch, but differing for the GaN buffer doping: Fe reference \rightarrow Fe = $2 \times 10^{18}\ \text{cm}^{-3}$, no C; Fe + low C \rightarrow Fe = $2 \times 10^{18}\ \text{cm}^{-3}$, C = $2 \times 10^{16}\ \text{cm}^{-3}$; Fe + high C \rightarrow Fe = $2 \times 10^{18}\ \text{cm}^{-3}$, C = $8 \times 10^{16}\ \text{cm}^{-3}$. 24 h test at $V_{GS} = -2\ \text{V}$, $V_{DS} = 25\ \text{V}$. Reproduced with permission.^[54] Copyright 2020, Elsevier.

negligible for the Fe-doped reference ones. For C-doped devices, the degradation consists in a decrease in transconductance and in a positive threshold voltage shift, while Fe-doped ones present only a negative V_{TH} shift. The presence of C in the GaN buffer induces therefore short-term reliability issues or “memory” effects, which can be relevant for some applications. In the tested $0.15\ \mu\text{m}$ devices, these memory effects become relevant when V_{DS} exceeds 25 V in semi-on state, as shown in Figure 13.

The different behavior of C-doped devices can be explained as follows: C_N deep levels behave as deep acceptors 0.8–0.9 eV from the valence band. When the devices are submitted to hot-electron tests in semi-on state or on-state, electrons may recombine at acceptor site, leaving an uncompensated acceptor, negatively charged; the consequent backgating effect decreases I_D and induces a positive threshold voltage shift. The effect can be recovered only when new holes are injected and compensate the negative charge; the recovery is therefore extremely slow and the degradation is semi-permanent. On the contrary, only trapping of electrons at deep levels at 0.6 eV from conduction band takes place in Fe-doped devices, resulting in relatively fast (0.1–1 ms typically) recovery times.

3. Conclusions

Failure modes and mechanisms of $0.15\text{--}0.5\ \mu\text{m}$ AlGaIn/GaN HEMTs have been reviewed. The main factors leading to the possible degradation of the devices are the individual or combined effects of current flow, electric field, and temperature, causing immediate or time-dependent (percolation) mechanical damage,

element diffusion, chemical reactions, and generation of defects. As gate length is scaled, a complex trade-off is created among short-channel effects, device stability and reliability, and frequency dispersion effects, requiring optimization of compensation dopants concentration and profile, and careful design of epitaxial structures, possibly with the introduction of new materials and double heterojunctions. Crystal damage due to thermomechanical stress can be limited by improving device thermal characteristics and reducing junction temperature; (Al)GaN oxidation remains an issue, but device robustness against this mechanism can be greatly improved by process optimization. Hot-electron-induced degradation may become the dominant failure mechanism for highly scaled devices; for $L_G = 100\ \text{nm}$ and below wider reliability, studies are needed to guarantee extended lifetime to future telecommunication systems.

Acknowledgements

Work partially supported by the Italian Ministry of Research project “Empowering GaN-on-SiC and GaN-on-Si technologies for the next challenging millimeter-wave applications,” GANAPP; by the European Space Agency project RELGAN, (supervisor of Jouni Latti); by the USA. Office of Naval Research (supervisor Paul Maki); by the European Commission ECSEL initiative project 5G_GaN2; by the European Defense Agency project EUGANIC.

Open Access Funding provided by Universita degli Studi di Padova within the CRUI-CARE Agreement.

Conflict of Interest

The authors declare no conflict of interest.

Keywords

degradation, failure mechanisms, gallium nitride, HEMTs, microwave, millimeter-wave, reliability

Received: October 24, 2021

Revised: February 13, 2022

Published online: November 19, 2022

- [1] R. Quay, M. Dammann, T. Kemmer, P. Brückner, M. Cwiklinski, D. Schwantuschke, S. Krause, S. Leone, M. Mikulla, *IEEE Int. Electron Device Meeting*, IEEE, Piscataway, NJ **2019**, pp. 394–397.
- [2] S. Din, et al., *2015 IEEE MTT-S Int. Microwave Symp. IMS*, IEEE, Piscataway, NJ **2015**, 28–31, <https://doi.org/10.1109/MWSYM.2015.7166776>.
- [3] K. Brown, et al., *2015 IEEE MTT-S Int. Microwave Symp. IMS 2015*, IEEE, Piscataway, NJ **2015**, pp. 1–3, <https://doi.org/10.1109/MWSYM.2015.7166801>.
- [4] D. Bisi, M. Meneghini, C. De Santi, A. Chini, M. Dammann, P. Bruckner, M. Mikulla, G. Meneghesso, E. Zanoni, *IEEE Trans. Electron Devices* **2013**, *60*, 3166.
- [5] N. Zagni, A. Chini, F. M. Puglisi, M. Meneghini, G. Meneghesso, E. Zanoni, P. Pavan, G. Verzellesi, *IEEE Trans. Electron Devices* **2021**, *68*, 697.
- [6] M. H. Wong, S. Keller, N. S. Dasgupta, D. J. Denninghoff, S. Kolluri, D. F. Brown, J. Lu, N. A. Fichtenbaum, E. Ahmadi, U. Singiseti,

- A. Chini, S. Rajan, S. P. Denbaars, J. S. Speck, U. K. Mishra, *Semicond. Sci. Technol.* **2013**, 28, 74009.
- [7] B. Romanczyk, S. Wienecke, M. Guidry, H. Li, E. Ahmadi, X. Zheng, S. Keller, U. K. Mishra, *IEEE Trans. Electron Devices* **2018**, 65, 45.
- [8] B. Romanczyk, M. Guidry, X. Zheng, P. Shrestha, H. Li, E. Ahmadi, S. Keller, U. K. Mishra, *Appl. Phys. Lett.* **2021**, 119, 072105.
- [9] W. Liu, B. Romanczyk, M. Guidry, N. Hatui, C. Wurm, W. Li, P. Shrestha, X. Zheng, S. Keller, U. K. Mishra, *IEEE Microwave Wireless Compon. Lett.* **2021**, 31, 748.
- [10] J. Scarpulla, *IEEE Int. Reliability Physics Symp. Proc.*, March 2021, Group C, <https://doi.org/10.1109/IRPS46558.2021.9405226>.
- [11] G. Meneghesso, G. Verzellesi, F. Danesin, F. Rampazzo, F. Zanon, A. Tazzoli, M. Meneghini, E. Zanoni, *IEEE Trans. Device Mater. Reliab.* **2008**, 8, 332.
- [12] E. Zanoni, et al., *Proc. MIKON 2016*, IEEE, Krakow, Poland **2016**, <https://doi.org/10.1109/mikon.2016.7492013>.
- [13] G. Meneghesso, M. Meneghini, A. Tazzoli, N. Ronchi, A. Stocco, A. Chini, E. Zanoni, *Int. J. Microwave Wireless Technol.* **2010**, 2, 39.
- [14] E. Zanoni, et al., *IEEE Int. Reliability Physics Symp. Proc.*, IEEE, Piscataway, NJ, April 2020, <https://doi.org/10.1109/IRPS45951.2020.9128358>.
- [15] J. A. Del Alamo, E. S. Lee, *IEEE Trans. Electron Devices* **2019**, 66, 4578.
- [16] M. G. Ancona, S. C. Binari, D. Meyer, *Phys. Status Solidi C* **2011**, 8, 2276.
- [17] M. G. Ancona, S. C. Binari, D. J. Meyer, *J. Appl. Phys.* **2012**, 111, 074504.
- [18] T. L. Wu, et al., *IEEE Int. Reliability Physics Symp. Proc.*, IEEE, Piscataway, NJ, May 2015, pp. 6C41–6C46, <https://doi.org/10.1109/IRPS.2015.7112769>.
- [19] M. Meneghini, A. Stocco, M. Bertin, D. Marcon, A. Chini, G. Meneghesso, E. Zanoni, *Appl. Phys. Lett.* **2012**, 100, 033505.
- [20] D. Marcon, et al., *Tech. Dig. - Int. Electron Devices Meeting IEDM*, 2010, pp. 472–475, <https://doi.org/10.1109/IEDM.2010.5703398>.
- [21] M. Meneghini, et al., *Tech. Dig. - Int. Electron Devices Meeting IEDM*, **2011**, pp. 469–472, <https://doi.org/10.1109/IEDM.2011.6131586>.
- [22] C. De Santi, M. Meneghini, M. Buffolo, G. Meneghesso, E. Zanoni, *IEEE Electron Device Lett.* **2016**, 37, 611.
- [23] M. Meneghini, I. Rossetto, F. Hurkx, J. Sonsky, J. A. Croon, G. Meneghesso, E. Zanoni, *IEEE Trans. Electron Devices* **2015**, 62, 2549.
- [24] I. Rossetto, M. Meneghini, S. Pandey, M. Gajda, G. A. M. Hurkx, J. A. Croon, J. Sonsky, G. Meneghesso, E. Zanoni, *IEEE Trans. Electron Devices* **2017**, 64, 73.
- [25] I. Rossetto, M. Meneghini, C. De Santi, S. Pandey, M. Gajda, G. A. M. Hurkx, J. Croon, J. Sonsky, G. Meneghesso, E. Zanoni, *IEEE Trans. Electron Devices* **2018**, 65, 1303.
- [26] E. Zanoni, M. Meneghini, G. Meneghesso, D. Bisi, I. Rossetto, A. Stocco, *3rd IEEE Work. Wide Band Gap Devices Appl.*, IEEE, Piscataway, NJ, **2015**, pp. 75–80.
- [27] J. Hu, S. Stoffels, M. Zhao, A. N. Tallarico, I. Rossetto, M. Meneghini, X. Kang, B. Bakeroot, D. Marcon, B. Kaczer, S. Decoutere, G. Groeseneken, *IEEE Electron Device Lett.* **2017**, 38, 371.
- [28] M. Dammann, et al., *IEEE Int. Integrated Reliability Workshop Final Rep.*, IEEE, Piscataway, NJ, February 2015, pp. 115–118, **2014**, <https://doi.org/10.1109/IIRW.2014.7049524>.
- [29] M. Dammann, M. Baeumler, V. Polyakov, P. Brückner, H. Konstanzer, R. Quay, M. Mikulla, A. Graff, M. Simon-Najasek, *Microelectron. Reliab.* **2017**, 76–77, 292.
- [30] M. Dammann, M. Baeumler, P. Brückner, W. Bronner, S. Maroldt, H. Konstanzer, M. Wespel, R. Quay, M. Mikulla, A. Graff, M. Lorenzini, M. Fagerlind, P. J. Van Der Wel, T. Roedle, *Microelectron. Reliab.* **2015**, 55, 1667.
- [31] M. Dammann, et al., in *2021 IEEE Int. Reliability Physics Symposium (IRPS)*, IEEE, Piscataway, NJ, March 2021, pp. 1–7, <https://doi.org/10.1109/IRPS46558.2021.9405227>.
- [32] F. Gao, S. C. Tan, J. A. Del Alamo, C. V. Thompson, T. Palacios, *IEEE Trans. Electron Devices* **2014**, 61, 437.
- [33] F. Gao, C. V. Thompson, J. Del Alamo, T. Palacios, in *Proc. CS MANTECH Conf.*, Denver CO, May 2014, pp. 29–32.
- [34] P. G. Whiting, M. R. Holzworth, A. G. Lind, S. J. Pearton, K. S. Jones, L. Liu, T. S. Kang, F. Ren, Y. Xin, *Microelectron. Reliab.* **2017**, 70, 32.
- [35] P. G. Whiting, N. G. Rudawski, M. R. Holzworth, S. J. Pearton, K. S. Jones, L. Liu, T. S. Kang, F. Ren, *Microelectron. Reliab.* **2012**, 52, 2542.
- [36] D. J. Cheney, E. A. Douglas, L. Liu, C. F. Lo, Y. Y. Xi, B. P. Gila, F. Ren, D. Horton, M. E. Law, D. J. Smith, S. J. Pearton, *Semicond. Sci. Technol.* **2013**, 28, 074019.
- [37] A. Sozza, et al., in *IEEE Int. Electron Devices Meeting, 2005. Digest.*, **2005**, pp. 590–593.
- [38] A. Sozza, C. Dua, E. Morvan, B. Grimber, S. L. Delage, *Microelectron. Reliab.* **2005**, 45, 1617.
- [39] M. Meneghini, A. Stocco, R. Silvestri, G. Meneghesso, E. Zanoni, *Appl. Phys. Lett.* **2012**, 100, 233508.
- [40] Y. S. Puzyrev, T. Roy, M. Beck, B. R. Tuttle, R. D. Schrimpf, D. M. Fleetwood, S. T. Pantelides, *J. Appl. Phys.* **2011**, 109, 034501.
- [41] M. Meneghini, I. Rossetto, D. Bisi, A. Stocco, A. Chini, A. Pantellini, C. Lanzieri, A. Nanni, G. Meneghesso, E. Zanoni, *IEEE Trans. Electron Devices* **2014**, 61, 4070.
- [42] D. Bisi, A. Chini, F. Soci, A. Stocco, M. Meneghini, A. Pantellini, A. Nanni, C. Lanzieri, P. Gamarra, C. Lacam, M. Tordjman, M.-A. Di-Forte-Poisson, G. Meneghesso, E. Zanoni, *IEEE Electron Device Lett.* **2015**, 36, 1011.
- [43] T. Roy, Y. S. Puzyrev, B. R. Tuttle, D. M. Fleetwood, R. D. Schrimpf, D. F. Brown, U. K. Mishra, S. T. Pantelides, *Appl. Phys. Lett.* **2010**, 96, 133503.
- [44] Y. S. Puzyrev, B. R. Tuttle, R. D. Schrimpf, D. M. Fleetwood, S. T. Pantelides, *Appl. Phys. Lett.* **2010**, 96, 053505.
- [45] E. Zanoni, M. Manfredi, S. Bigliardi, A. Paccagnella, P. Pisoni, C. Tedesco, C. Canali, *IEEE Trans. Electron Devices* **1992**, 39, 1849.
- [46] D. Bisi, C. De Santi, M. Meneghini, S. Wienecke, M. Guidry, H. Li, E. Ahmadi, S. Keller, U. K. Mishra, G. Meneghesso, E. Zanoni, *IEEE Electron Device Lett.* **2018**, 39, 1007.
- [47] M. Meneghini, A. Stocco, N. Ronchi, F. Rossi, G. Salviati, G. Meneghesso, E. Zanoni, *Appl. Phys. Lett.* **2010**, 97, 063508.
- [48] M. Rzin, M. Meneghini, F. Rampazzo, V. G. Zhan, D. Marcon, J. Grunenputt, H. Jung, B. Lambert, K. Riepe, H. Blanck, A. Graff, F. Altmann, M. Simon-Najasek, D. Poppitz, G. Meneghesso, E. Zanoni, *IEEE Trans. Electron Devices* **2020**, 67, 2765.
- [49] D. Floriot, H. Blanck, D. Bouw, F. Bourgeois, M. Camiade, L. Favède, M. Hosch, H. Jung, B. Lambert, A. Nguyen, K. Riepe, J. Spletstöß, H. Stieglaue, J. Thorpe, U. Meiners, in *European Microwave Week 2012: "Space for Microwaves"*, *EuMW 2012, Conf. Proc. - 7th European Microwave Integrated Circuits Conf., EuMIC 2012*, **2012**, pp. 317–320.
- [50] L. Brunel, B. Lambert, P. Mezenge, J. Bataille, D. Floriot, J. Grunenputt, H. Blanck, D. Carisetti, Y. Gourdel, N. Malbert, A. Curutchet, N. Labat, *Microelectron. Reliab.* **2013**, 53, 1450.

- [51] Y. Puzyrev, A. Paccagnella, S. T. Pantelides, S. Mukherjee, J. Chen, T. Roy, M. Silvestri, R. D. Schrimpf, D. M. Fleetwood, J. Singh, J. M. Hinkley, *IEEE Trans. Electron Devices* **2014**, *61*, 1316.
- [52] J. He, Y. Q. Chen, Z. Y. He, Y. F. En, C. Liu, Y. Huang, Z. Li, M. H. Tang, *IEEE J. Electron Devices Soc.* **2019**, *7*, 76.
- [53] M. J. Uren, M. Kuball, *Jpn. J. Appl. Phys.* **2021**, *60*, SB0802.
- [54] Z. Gao, F. Rampazzo, M. Meneghini, C. De Santi, F. Chiocchetta, D. Marcon, G. Meneghesso, E. Zanoni, *Microelectron. Reliab.* **2020**, *114*, 113905.



Enrico Zanoni is professor of microelectronics at the Department of Information Engineering of the University of Padova since 1993 and an IEEE Fellow since 2009. At the University of Padova, he contributed to establish a research group involved in CMOS analog and rf-integrated circuit design, CMOS reliability and radiation hardness, compound semiconductor characterization, modeling, and reliability. Enrico Zanoni is coauthor of more than 800 publications on the modeling and reliability physics of silicon and compound semiconductor devices and of 4 patents.



Fabiana Rampazzo received a degree in physics from the University of Padova working on characterization and reliability of M.O.S. capacitors with Silicon Carbide substrate. In 2005, she received the Ph.D. degree in electronics and telecommunications engineering studying current instabilities, passivation effects, and other reliability aspects in AlGaIn/GaN HEMTs for Microwave applications. She is working now as laboratory assistant in the same university. Her main research topics include the characterization of microwave devices on III–V semiconductors such as GaN, GaAs, and InP, with particular aim to transient phenomena; electrical characterization of electronic devices grown on wide bandgap semiconductors (SiC and GaN); reliability studies of the long-term stability of microwave devices with particular attention to their failure mode and mechanisms with also the help of SEM and FIB.



Carlo De Santi, since September 2019, holds an assistant professor position at the University of Padova. His main research activities focus on the characterization, modeling of physical processes, and reliability of electronic and optoelectronic devices based on elemental and compound semiconductors, including various ternary and quaternary compounds. The application fields of interest are power electronics and radio frequency systems, LEDs and lasers in the UV, visible monochromatic and white spectral range, devices for silicon photonics, solar cells and photodetectors, and phosphors and systems for lighting applications. He is a co-author of more than 250 journal and conference papers, including 43 invited ones.



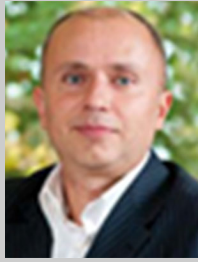
Veronica Gao Zhan received her Bachelor of Science and Bachelor of Literature degrees (2008) from the Harbin Institute of Technology (HIT), her Master of Science degree (2011) from Beijing Jiaotong University (BJTU), and her Ph.D. degree on electronic engineering from Instituto de Sistemas Optoelectrónica y Microtecnología in Universidad Politécnica de Madrid (ISOM-UPM), now she is working on defects and reliability study of GaN-based HEMTs in Dipartimento di Ingegneria Dell'informazione (Dei) in Università degli Studi di Padova (UNIPD).



Chandan Sharma has done his Ph.D. from the department of Physics, Indian Institute of Technology Delhi, India. He has also worked as research scholar in the MMIC Fabrication division, Solid State Physics Laboratory Delhi, India. During his Ph.D., he worked on fabrication and DC/pulse characterization of GaN material-based HEMT devices. He also went to National Chiao Tung University (NCTU), Taiwan where he worked under Prof. Tian-li Wu on Reliability of various AlGaIn/GaN HEMTs and MISHEMTs. His research interest includes III–V semiconductor materials and reliability studies on AlGaIn/GaN-based HEMT devices.



Nicola Modolo was born in Venice, Italy. He received the Master's degree (Cum Laude) in electronic engineering from Università degli Studi di Padova, Padova, Italy, in 2019. From February 2018, to June 2019, he completed the Exchange Student program, and worked as Short-Term Inbound Researcher at the National Chiao Tung University, Hsinchu, Taiwan, in the International College of Semiconductor Technology. He is currently working as Ph.D. student with ACME Lab at Università degli Studi di Padova where he is studying reliability and degradation mechanisms of Power GaN HEMTs under static and dynamic stress conditions. The research program is partnered with Infineon Technologies, Villach, Austria.



Giovanni Verzellesi received the "Laurea" degree in electrical engineering from the University of Bologna, Bologna, Italy, in 1989, and the Ph.D. degree also in electrical engineering from the University of Padova, Padova, Italy, in 1994. In 1993–1994, he was a visiting graduate student with the University of California, Santa Barbara (CA, USA). From 1994 to 1999, he was with the University of Trento, Italy, as an assistant professor of Electronics. Since 1999, he has been with the University of Modena and Reggio Emilia, Italy, where he became associate professor in 2000 and professor in 2006.



Alessandro Chini received the Laurea degree and the Ph.D. degree from the Università di Padova, Padova, Italy, in 1999 and 2003, respectively. From 2002 to 2004, he was an assistant research engineer with the University of California, Santa Barbara. Since 2004, he has been with the Università di Modena e Reggio Emilia, Modena, Italy, where he is currently an associate professor with the Dipartimento di Ingegneria "Enzo Ferrari." His current research interests include the characterization, failure mechanisms investigation, and TCAD modeling of wide bandgap semiconductor-based devices.



Gaudenzio Meneghesso (IEEE S'95–M'97–SM'07–F'13) graduated in electronics engineering at the University of Padova in 1992 working on the failure mechanism induced by hot electrons in MESFETs and HEMTs. Since 2011, he is with University of Padova as full professor. His research interests involve mainly the electrical characterization, modeling, and reliability of microelectronics devices. Within these activities, he published more than 800 technical papers (of which more than 100 Invited Papers and 12 best paper awards). He has been nominated to IEEE Fellow class 2013, with the following citation: "for contributions to the reliability physics of compound semiconductor devices."



Matteo Meneghini received his Ph.D. in electronic and telecommunication engineering (University of Padova), working on the optimization of GaN-based LED and laser structures. Currently, he is an associate professor at the Department of Information Engineering, University of Padova. His main interest is the characterization, reliability, and modeling of compound semiconductor devices (LEDs, laser diodes, HEMTs), and optoelectronic components, including solar cells. Within these activities, he has published more than 400 journal and conference proceedings papers.